

# 押出成形 CAE における 新規 2.5D FEM 解析技術の活用と今後の展望

Applications of new 2.5D FEM Analysis Technology  
in Extrusion CAE and Future Prospects

2022/6/15

((株)HASL) ○谷藤 真一郎, 依藤 大輔

(芝浦機械(株)) 尾原 正俊

((株)プラスチック工学研究所) 鬼防 崇, 辰巳 昌典

(金沢大学) 瀧 健太郎

## Practical 2.5D FEM simulation for polymer extrusion process

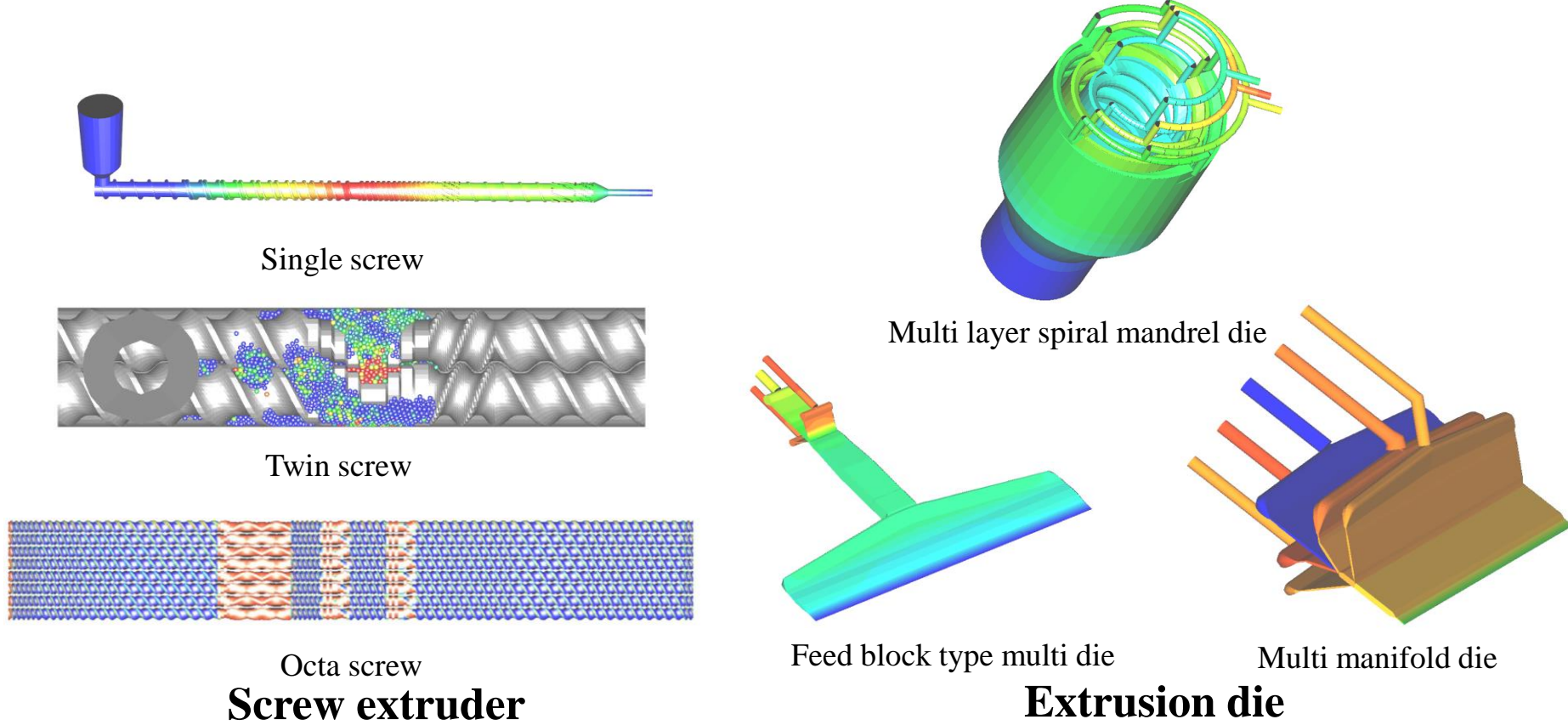


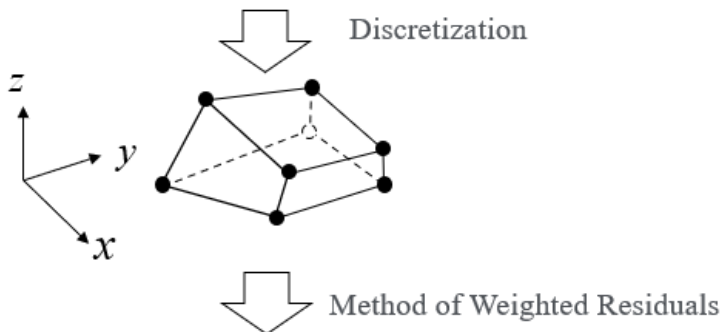
**Fig. 1 Various equipments used in the extrusion molding**

# □ Recently published papers concerning 2.5D FEM 3/30

- 1) Ohara, M., Tanifuji, S., Sasai, Y., Sugiyama, T., Umemoto, S.,  
Murata, J., Tsujimura, I., Kihara, S. and Taki, K. Twin Screw  
「Resin Distribution along Axial and Circumferential Directions of  
Self-Wiping Co-Rotating Parallel Twin-Screw Extruder」  
*AICHE J.*, **66**, 11, e17018(2020)
- 2) Ohara, M., Sasai, Y., Umemoto, S., Tanifuji, S., Kihara, S. and Taki, K. Twin Screw  
「Experimental and Numerical Simulation Study of Devolatilization  
in a Self-Wiping Corotating Parallel Twin-Screw Extruder」  
*Polymers*, **12**, 11, 2728(2020)
- 3) Tanifuji, S., Yorifuji, D., Kibou, T. and Tatsumi, M. Multi Layer Die  
「A Generalized 2.5D FEM Formulation for Steady Non-Newtonian Viscous Multi Flow  
Part 1: Formulation and Theoretical Verification」  
*Seikei-Kakou*, **33**, 2, 60(2021)
- 4) Tanifuji, S., Yorifuji, D., Kibou, T. and Tatsumi, M. Multi Layer Die  
「A Generalized 2.5D FEM Formulation for Steady Non-Newtonian Viscous Multi Flow  
Part 2: Implementation of Pseudo Encapsulation Model and Experimental Verification」  
*Seikei-Kakou*, **33**, 12, 447(2021)
- 5) Liu, C., Mikoshiba, S., Kobayashi, Y., Ishigami, A., Yorifuji, D.,  
Tanifuji, S. and Ito, H. Octa Screw  
「Experimental Investigation and Numerical Simulation  
of a Self-Wiping Corotating Parallel Octa-Screw Extruder」  
*Polymers*, **14**, 6, 1201(2022)

## 3D FEM

Stokes equation (Parabolic type)  
Continuity equation (Incompressible)



Weak form

$$\begin{pmatrix} \times & \times & \times & \times \\ \times & \times & \times & \times \\ \times & \times & \times & \times \\ \times & \times & \times & 0 \end{pmatrix} \begin{pmatrix} u \\ v \\ w \\ p \end{pmatrix} = \begin{pmatrix} \times \\ \times \\ \times \\ \times \end{pmatrix}$$

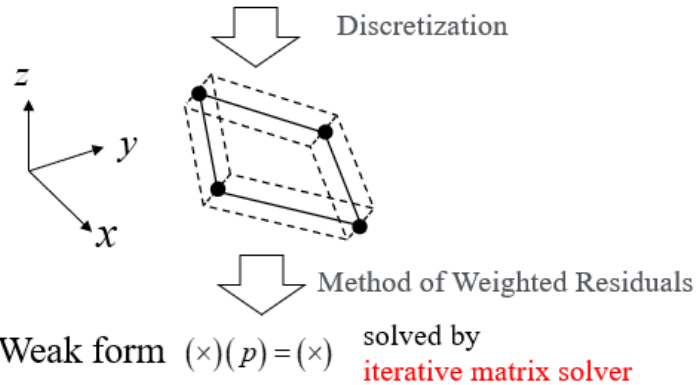
solved by direct matrix solver

## 2.5D FEM

Stokes equation (Parabolic type)  
Semi analytical integration

Semi analytical solution  
Continuity equation (Incompressible)

Averaging in thickness direction  
Pressure equation (Elliptic type)



$(u, v, w)$ : Flow velocity vector  
 $p$ : Flow pressure

**Fig. 2 Comparison of 3D and 2.5D FEM discretization procedures**

## □ Generalization of 2.5D FEM formulation

5/30

# Pressure equation

# **Original Form** since 1970'~(Cornell university)

# Flow analysis in injection molding

## Flow analysis in mono layer extrusion die

$$Q_\alpha = S_{\alpha\beta} p_\beta$$

↑ Flux                      ↑ Pressure gradient flow

## Generalized Form

# Generalization in semi analytical integration

## Flow analysis in screw extruder

$$Q_\alpha = S_{\alpha\beta} p_\beta + D_\alpha$$

↑  
Drag flow

## Flow analysis in multi layer extrusion die

$$Q_\alpha^l = S_{\alpha\beta}^l p_\beta^l + F_\alpha^l = 0 \text{ for } l=1 \sim n$$

↑  
Interaction flow with adjacent layers

$\alpha, \beta$ : Nodal number

$S_{\alpha\beta}$ : Flow conductance matrix     $D_\alpha, F_\alpha^l$ : Load vector

**Fig. 3 Generalized form of the pressure equation**

# Free (Layer) surface tracking method

## Multi purpose method

Eulerian method :

VOF

Level-Set

CIP

Arbitrary Lagrangian Eulerian method :

ALE

Particle method :

DEM

SPH

MPS

Free surface updated by using  
**flow velocity vector information**

## Problem oriented method in 2.5D FEM

Un-fill state in screw extruder :

Rearrangement of the pressure distribution

$$p(\theta, z) = p(\theta + \Delta\theta, z + \Delta z) - \frac{\partial p}{\partial \theta} \Delta\theta - \frac{\partial p}{\partial z} \Delta z$$

Multi layer surface :

Balance equation of the normal stress  
on multi layer surface

$$-p^I + 2\eta^I \frac{1}{h^I} \frac{Dh^I}{Dt} = -p^{II} + 2\eta^{II} \frac{1}{h^{II}} \frac{Dh^{II}}{Dt}$$

Free surface updated by using  
**flow pressure information**

**Fig. 4 Various free surface tracking methods**

## 「Resin Distribution along Axial and Circumferential Directions of Self-Wiping Co-Rotating Parallel Twin-Screw Extruder」<sup>1)</sup>



Experimental information



Numerical prediction

→  
Transport direction

Homo polypropylene (F-704NP)  
supplied by Prime Polymer (Japan)

Fig.5 Qualitative comparison of the resin fill distribution measured during the experiment and predicted by the simulation for 1 kg/h and 88 rpm

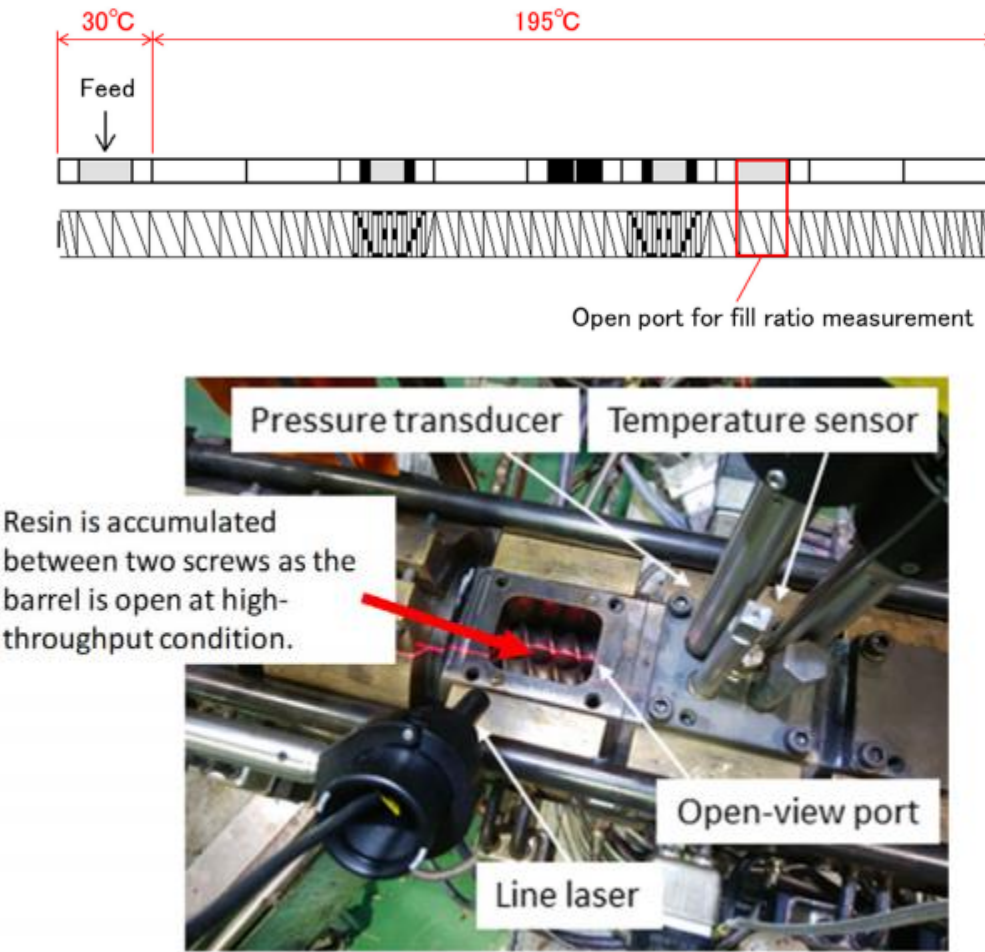
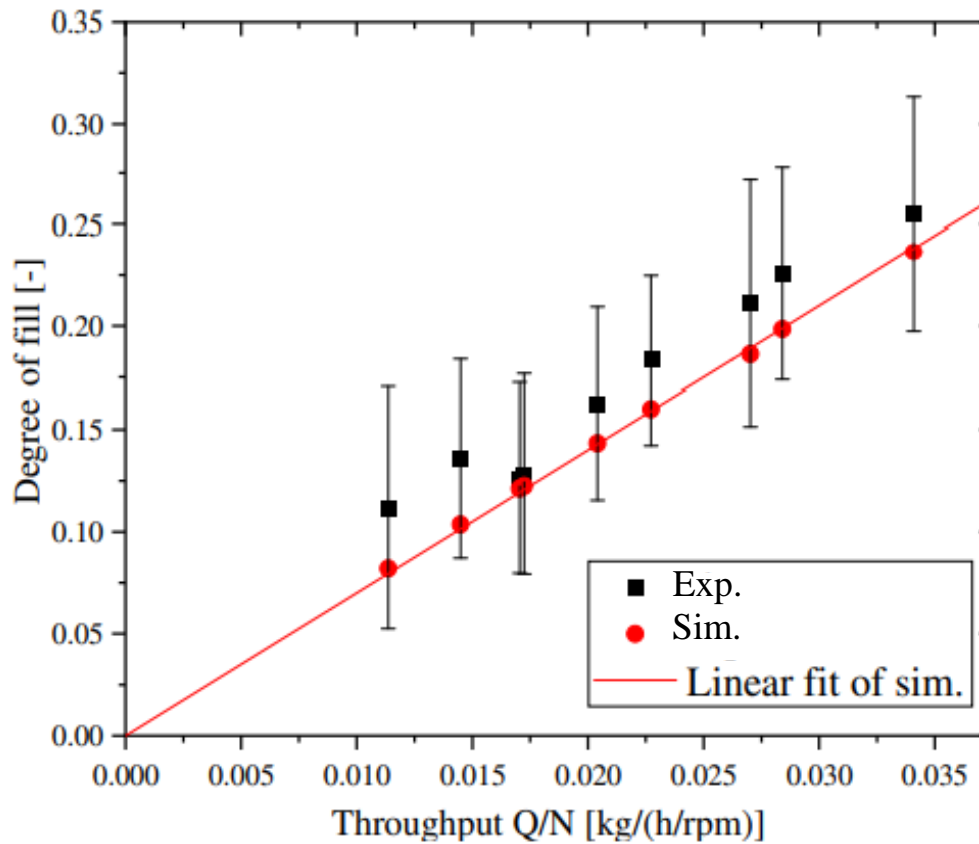


**Fig.6 Open-view port of TSE and line laser**



Theoretically

$$f = \frac{Q}{Q_d} = \frac{1}{g} \frac{Q}{N}$$

**Fig.7 Comparison of simulation and experimental results for the effect of throughput on the degree of fill**

# 「Experimental and Numerical Simulation Study of Devolatilization in a Self-Wiping Corotating Parallel Twin-Screw Extruder」<sup>2)</sup>

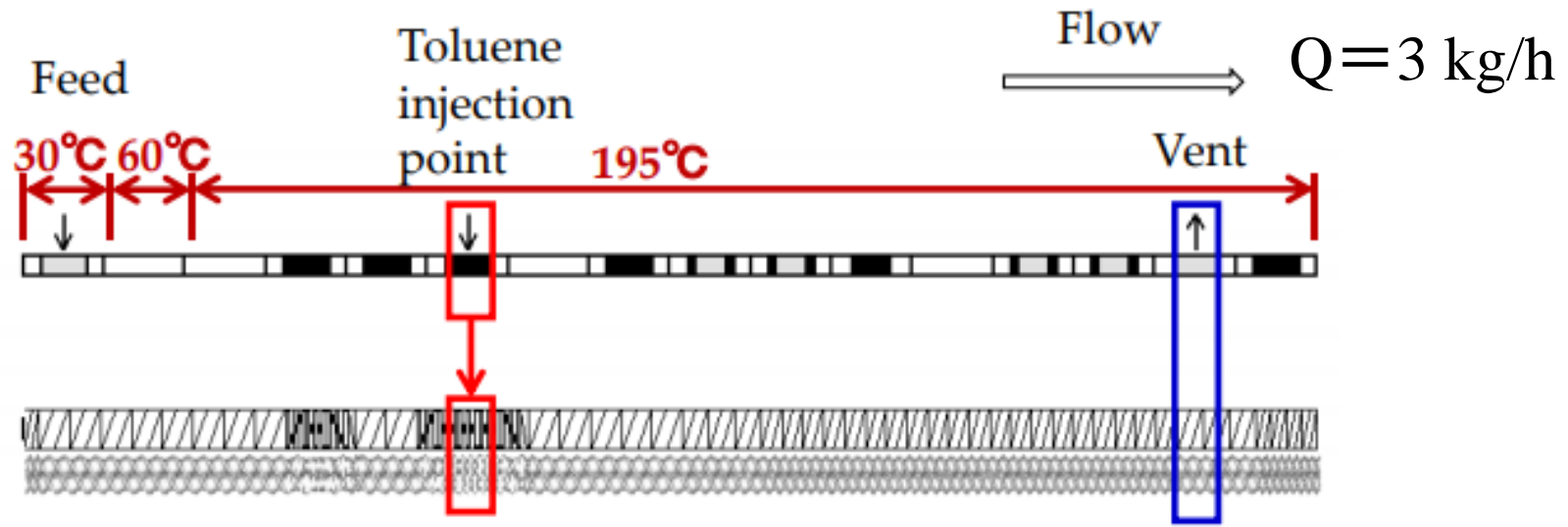
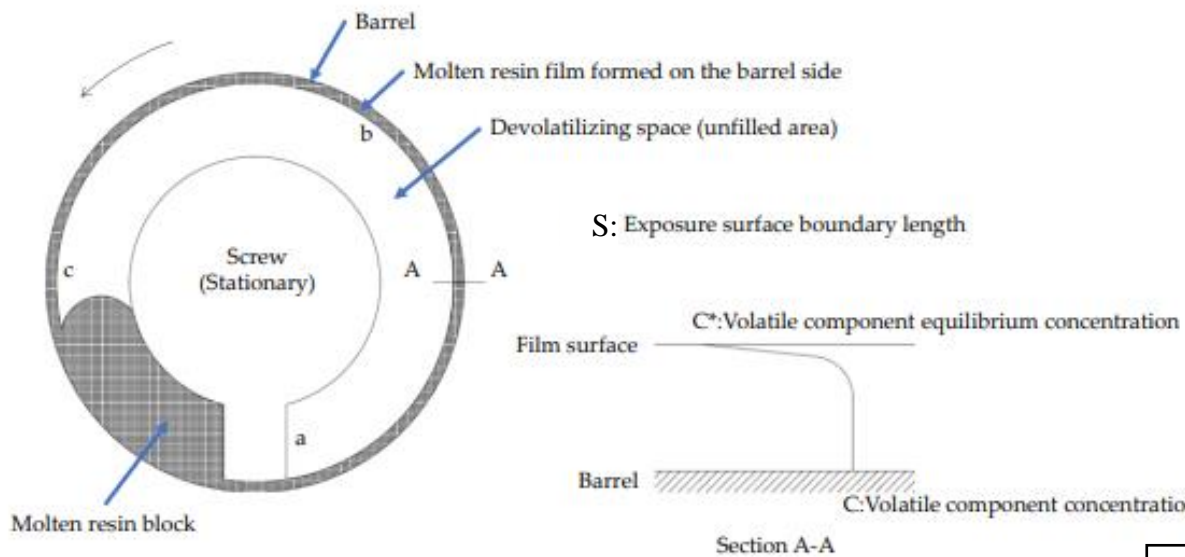


Fig.8 Screw configuration and barrel temperature settings



$$\chi = \frac{C(z_s) - C}{C(z_e) - C^*} = \exp \left( \frac{\rho_m}{Q_w} (SD_b D_m N)^{1/2} (z_e - z_s) \right)$$

**Fig.9 Schematic illustration of Latinen's model\*) for devolatilization in a single-screw extruder**

\*) Latinen, G.A. Devolatilization of viscous polymer systems. In Polymerization and Polycondensation Processes; American Chemical Society: Washington, DC, USA, 1962; Volume 34, pp. 235–246.

$\chi$ :	Devolatile efficiency
$z_e - z_s$ :	Partial fill interval
$\rho_m$ :	Melt density
$Q_w$ :	Mass flux
$D_b$ :	Barrel diameter
$D_m$ :	Diffusion coefficient
$N$ :	Rotation speed

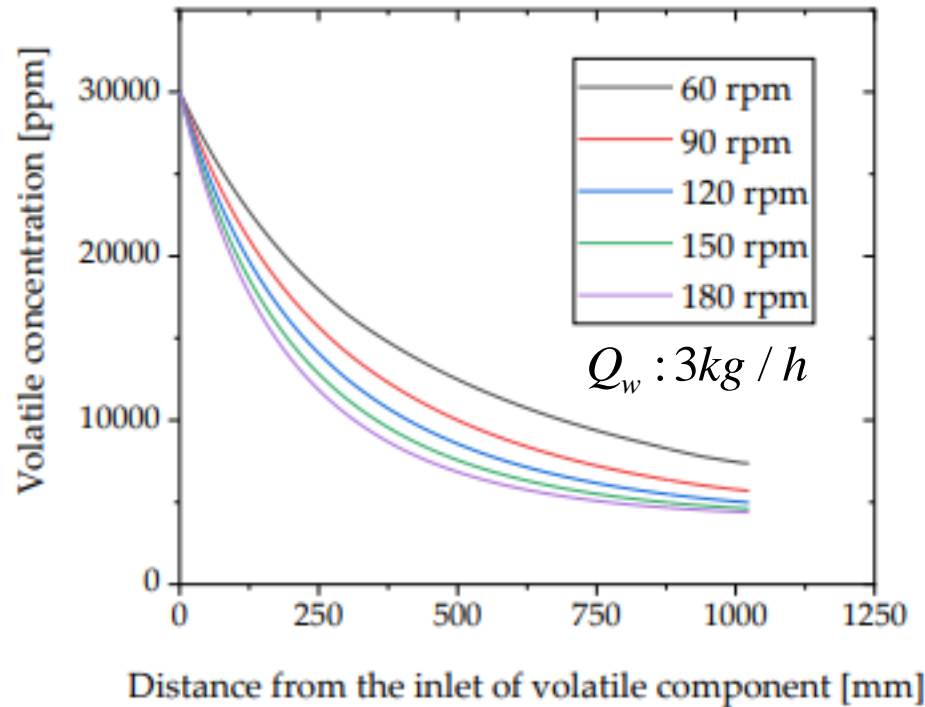


**Fig.10 Simulation results of toluene concentration along the machine direction of twin screw extruder**

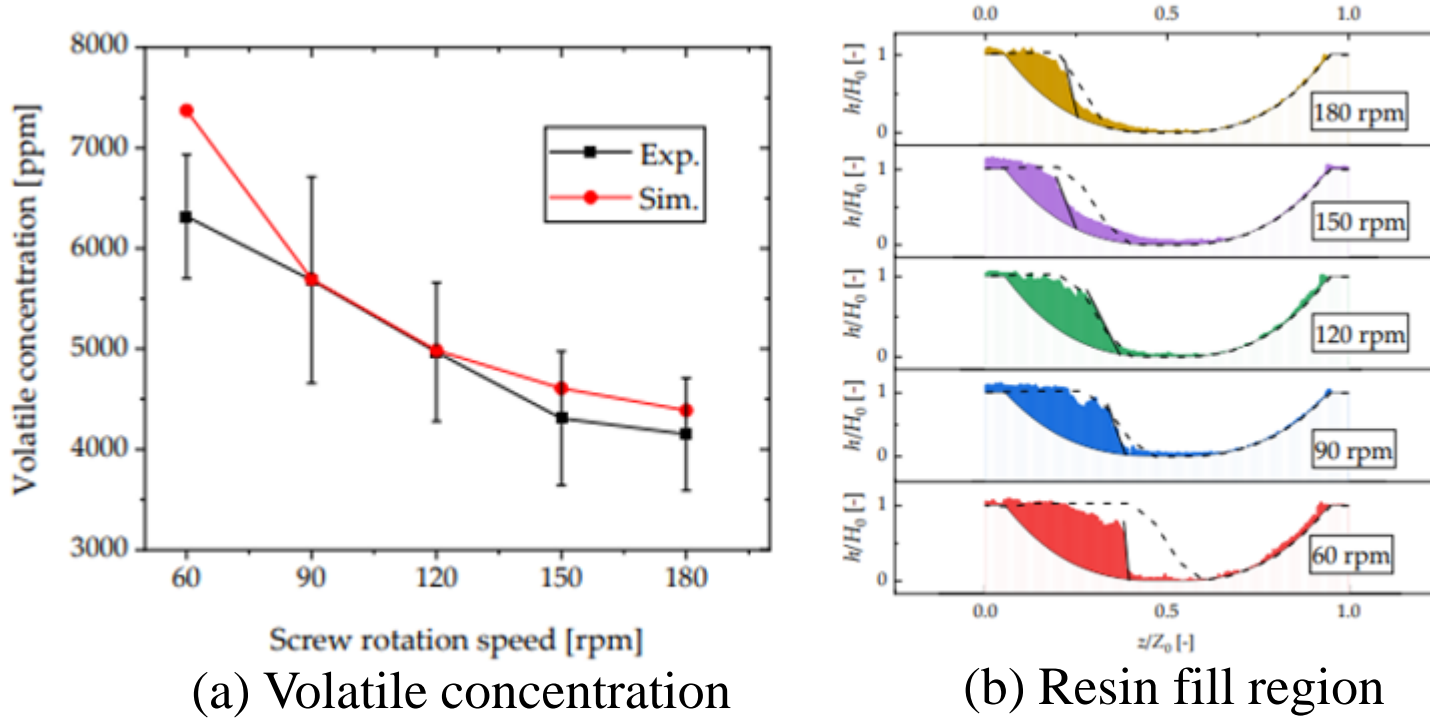
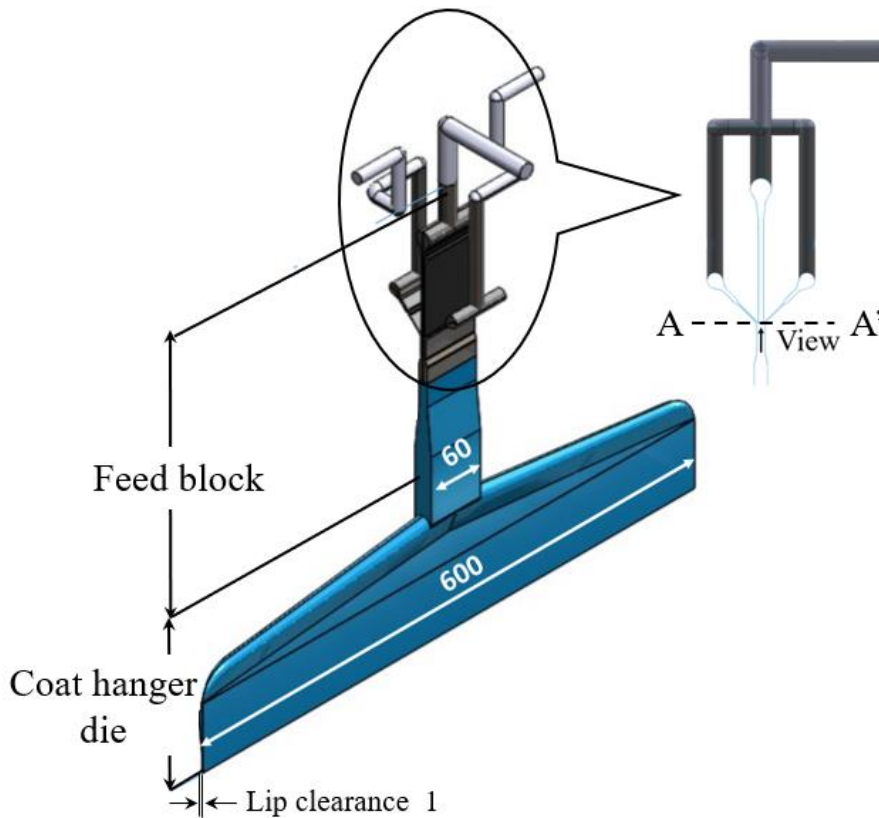


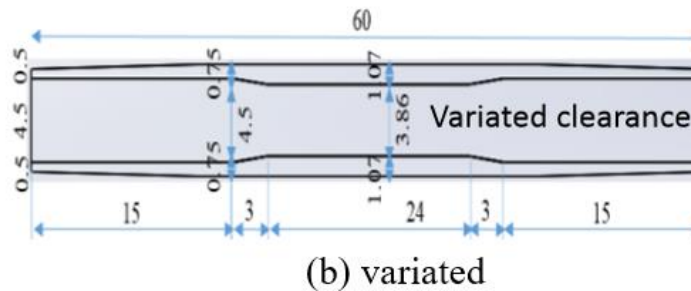
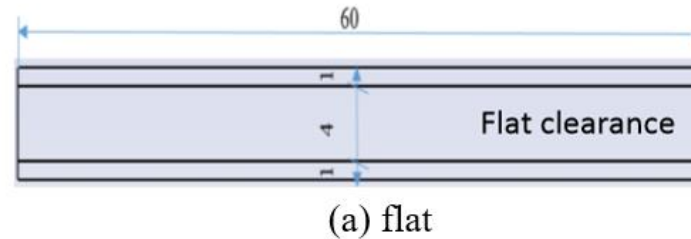
**Fig.11 Comparison of the experiment and the predicted information ((a) volatile concentration, (b) resin fill region)**

## 「A Generalized 2.5D FEM Formulation for Steady Non-Newtonian Viscous Multi Flow : Part 1 & 2」<sup>3),4)</sup>



Surface layer : LDPE (LC720), 4 kg/h, 215°C

Mid layer : LDPE (LF405M), 16 kg/h, 215°C



Scale unit : [mm]

Fig. 12 Feed block type coat hanger die used in the experimental verification

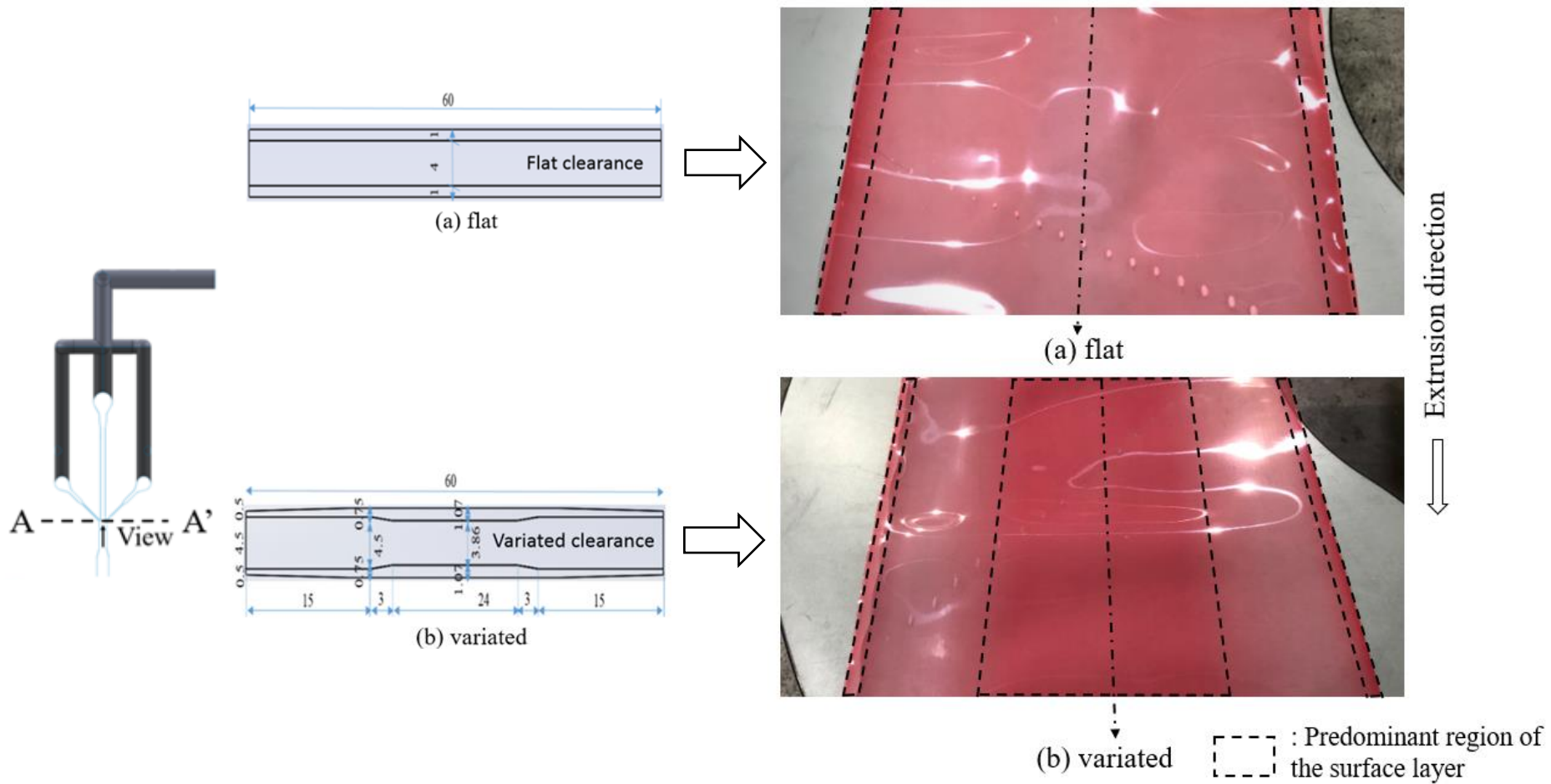
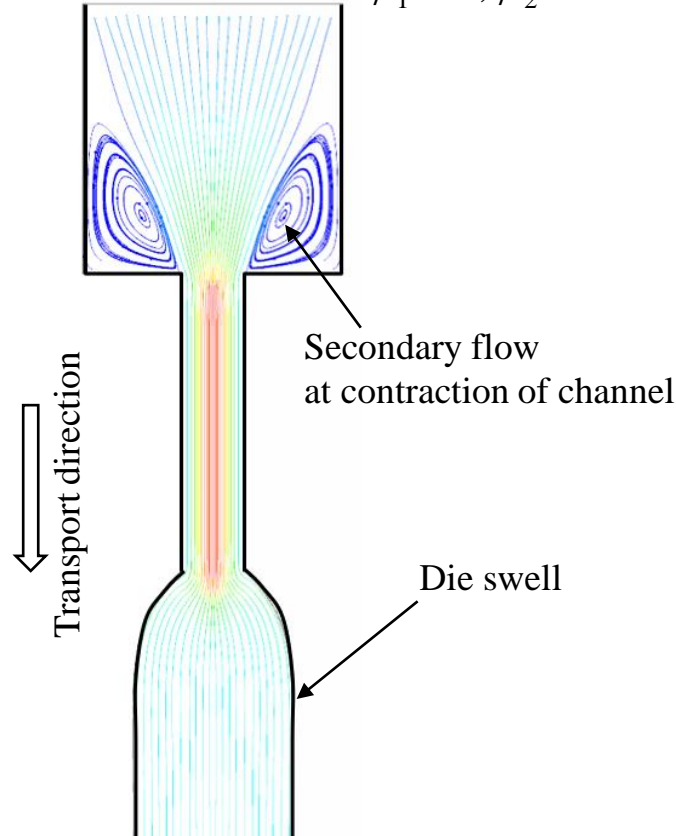


**Fig. 13 Snapshots of the extruded multilayer film  
((a) flat and (b) variated)**

# Viscoelastic phenomena neglected in the traditional 2.5D FEM

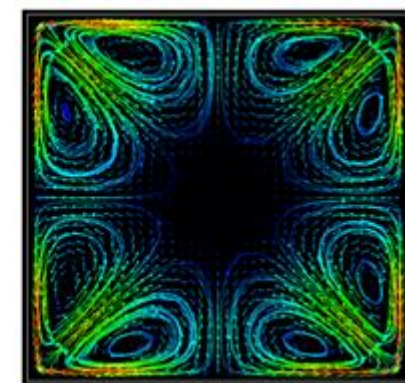
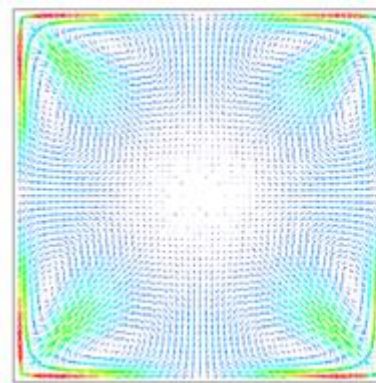
Main effecting factor :  
first normal stress difference

$$\psi_1 > 0, \psi_2 = 0$$



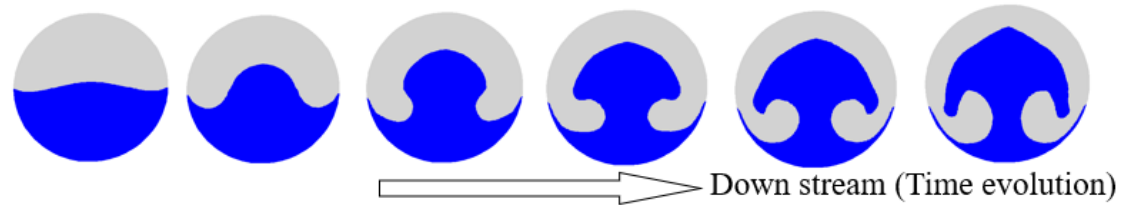
Main effecting factor :  
second normal stress difference

$$\psi_1 = 0, \psi_2 < 0$$



Transport  
direction

Secondary flow in the rectangular cross section channel



Variation of multi layer flow interface in the circular cross section channel  
(blue region : high viscosity flow, gray region : low viscosity flow )

**Fig. 14 Various viscoelastic phenomena**

# Derivation of Pseudo Encapsulation Model

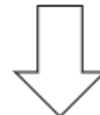
## Governing equations

Momentum equation for creep flow

$$\nabla \bullet \sigma = 0$$

CEF (Criminale Ericksen Filbey) model<sup>\*</sup>

$$\tau = 2\eta D - \psi_1 \overset{\nabla}{D} + 4\psi_2 D \bullet D$$



Steady state

$u \gg v, w$

Uniformity in machine direction

$$\frac{\partial \tau_{xx}}{\partial x} = \frac{\partial \tau_{xy}}{\partial x} = \frac{\partial \tau_{xz}}{\partial x} = 0$$

## Viscoelastic momentum equations

MD: Machine Direction

$$\frac{\partial p}{\partial x} = \frac{\partial \tau_{xx}}{\partial x} + \frac{\partial \tau_{xy}}{\partial y} + \frac{\partial \tau_{xz}}{\partial z} = \frac{\partial}{\partial y}(\eta \dot{\gamma}_{xy}) + \frac{\partial}{\partial z}(\eta \dot{\gamma}_{xz})$$

Equivalent to  
viscous fluid equation

Thickness Direction

$$\frac{\partial p}{\partial y} = \frac{\partial \tau_{xy}}{\partial x} + \frac{\partial \tau_{yy}}{\partial y} + \frac{\partial \tau_{yz}}{\partial z} = \frac{\partial}{\partial x}(\psi_2 \dot{\gamma}_{xy}^2) + \frac{\partial}{\partial z}(\psi_2 \dot{\gamma}_{xy} \dot{\gamma}_{xz})$$

TD: Transverse Direction

$$\frac{\partial p}{\partial z} = \frac{\partial \tau_{xz}}{\partial x} + \frac{\partial \tau_{yz}}{\partial y} + \frac{\partial \tau_{zz}}{\partial z} = \frac{\partial}{\partial y}(\psi_2 \dot{\gamma}_{xy} \dot{\gamma}_{xz}) + \frac{\partial}{\partial z}(\psi_2 \dot{\gamma}_{xz}^2)$$

Generates  
pressure gradient  
in each direction

$$\left\{ \begin{array}{l} \dot{\gamma}_{xy} = \frac{\partial u}{\partial y} \\ \dot{\gamma}_{xz} = \frac{\partial u}{\partial z} \end{array} \right.$$

\*) Criminale, Jr. W.O., Ericksen, J.L. and Filbey, Jr. G. L. :  
*Arch. Rat. Mech. Anal.*, **1**, 410(1985)

TD: Transverse Direction

$$\frac{\partial p}{\partial z} = \frac{\partial \tau_{xz}}{\partial x} + \frac{\partial \tau_{yz}}{\partial y} + \frac{\partial \tau_{zz}}{\partial z} = \frac{\partial}{\partial y} (\psi_2 \dot{\gamma}_{xy} \dot{\gamma}_{xz}) + \frac{\partial}{\partial z} (\psi_2 \dot{\gamma}_{xz}^2)$$

$\eta, \psi_2, H$  : constant

Averaging in thickness direction

Using analytical solution  
of mono layer flow

Approximate representation of pressure

$$\langle p(z) \rangle = \langle p(0) \rangle + \psi_2 \dot{\gamma}_w^2 g_f(z),$$

$$\dot{\gamma}_w = \left| \frac{W}{2\eta} \frac{\partial p}{\partial x} \right|,$$

$$g_f(z) = \frac{32}{\pi^4} \left( \frac{H}{W} \right)^2 \sum_{n=1}^{\infty} \frac{1}{(2n-1)^4} \left( \frac{\sinh \left( \frac{(2n-1)\pi z}{H} \right)}{\cosh \left( \frac{(2n-1)\pi W}{2H} \right)} \right)^2$$

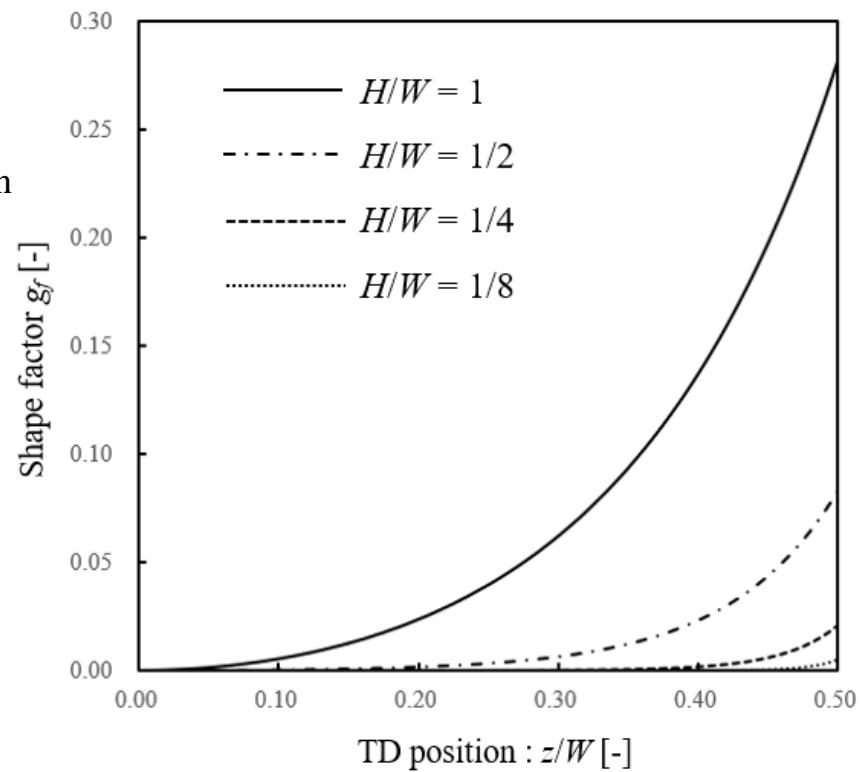
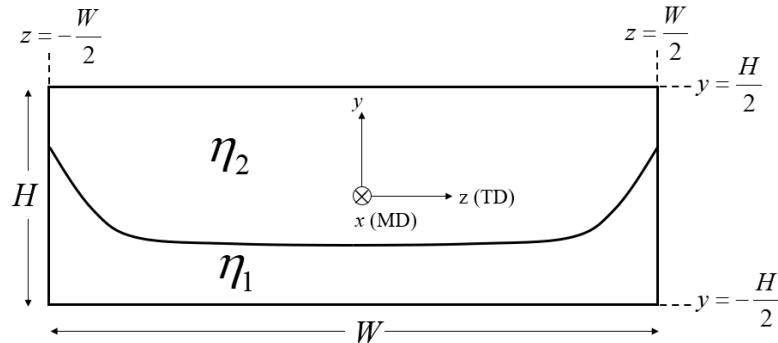


**Fig. 15 Dependency of aspect ratio and TD position for the shape factor :  $g_f$**

# Representation of the encapsulation using PEM



$$2\left(\frac{\eta_1}{h_1} + \frac{\eta_2}{h_2}\right)u \frac{\partial h_1}{\partial x} = p_1 - p_2 + \left(\psi_{2,2}\langle\dot{y}_{W2}^2\rangle - \psi_{2,1}\langle\dot{y}_{W1}^2\rangle\right)g_f(z)$$

$$\begin{cases} p_1 > p_2 \rightarrow \frac{\partial h_1}{\partial x} > 0 \\ p_1 < p_2 \rightarrow \frac{\partial h_1}{\partial x} < 0 \end{cases}$$

$$\begin{cases} \psi_{2,2}\left(\frac{1}{\eta_2} \frac{\partial p_2}{\partial x}\right)^2 > \psi_{2,1}\left(\frac{1}{\eta_1} \frac{\partial p_1}{\partial x}\right)^2 \rightarrow \frac{\partial h_1}{\partial x} > 0 \\ \psi_{2,2}\left(\frac{1}{\eta_2} \frac{\partial p_2}{\partial x}\right)^2 < \psi_{2,1}\left(\frac{1}{\eta_1} \frac{\partial p_1}{\partial x}\right)^2 \rightarrow \frac{\partial h_1}{\partial x} < 0 \end{cases}$$

**Assumption:**  $p_1 \approx p_2$ ,

$$\lambda = \frac{\eta_1}{\eta_2} \approx \frac{\psi_{2,1}}{\psi_{2,2}} < 1$$

?

$$\lambda^2 < \lambda \rightarrow \frac{\partial h_1}{\partial x} > 0$$

**Low-viscosity fluid encapsulates high-viscosity fluid under limited condition.**

!!!

## 2.5D FEM model

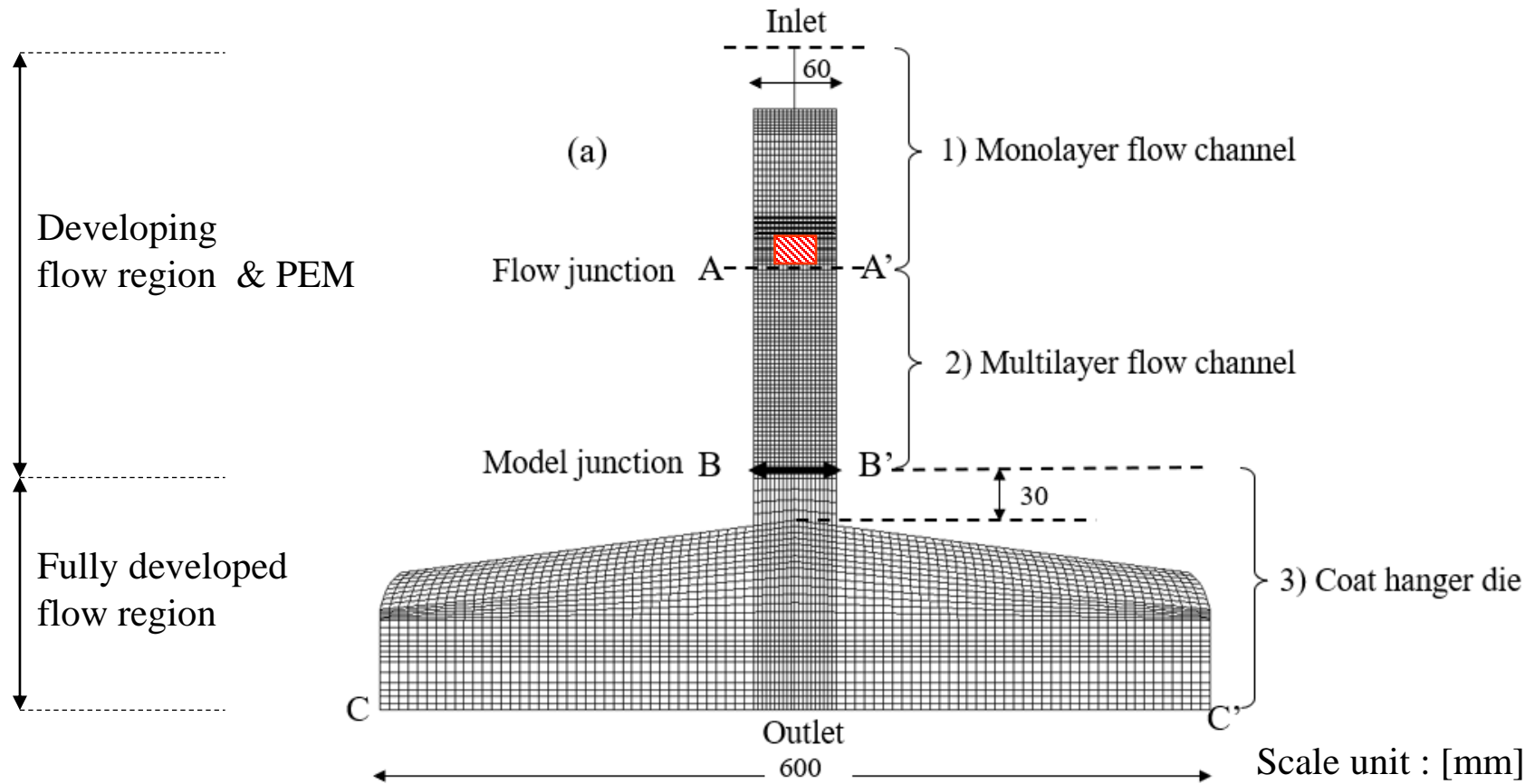
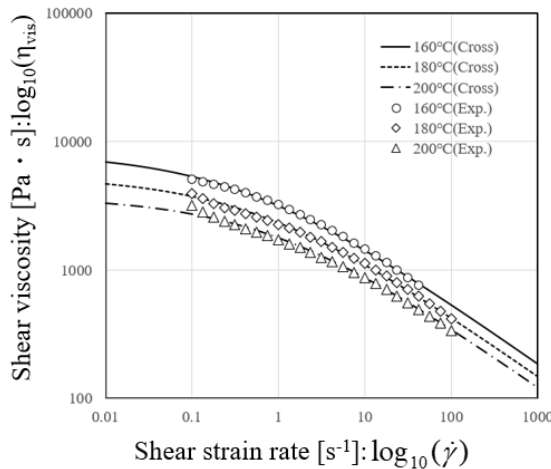


**Fig. 16 Multi layer flow analysis model**

# Material properties

(a) LC720  
Surface layer



(b) LF405M  
Mid layer

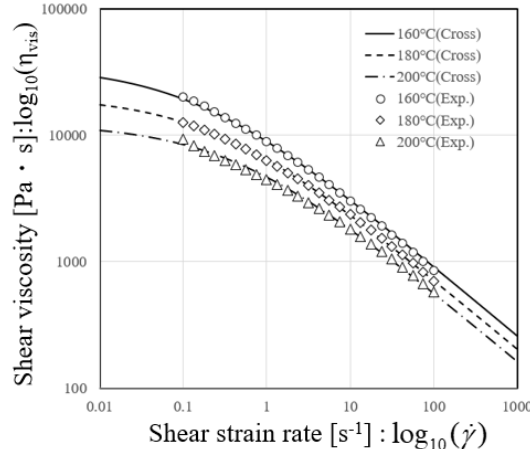
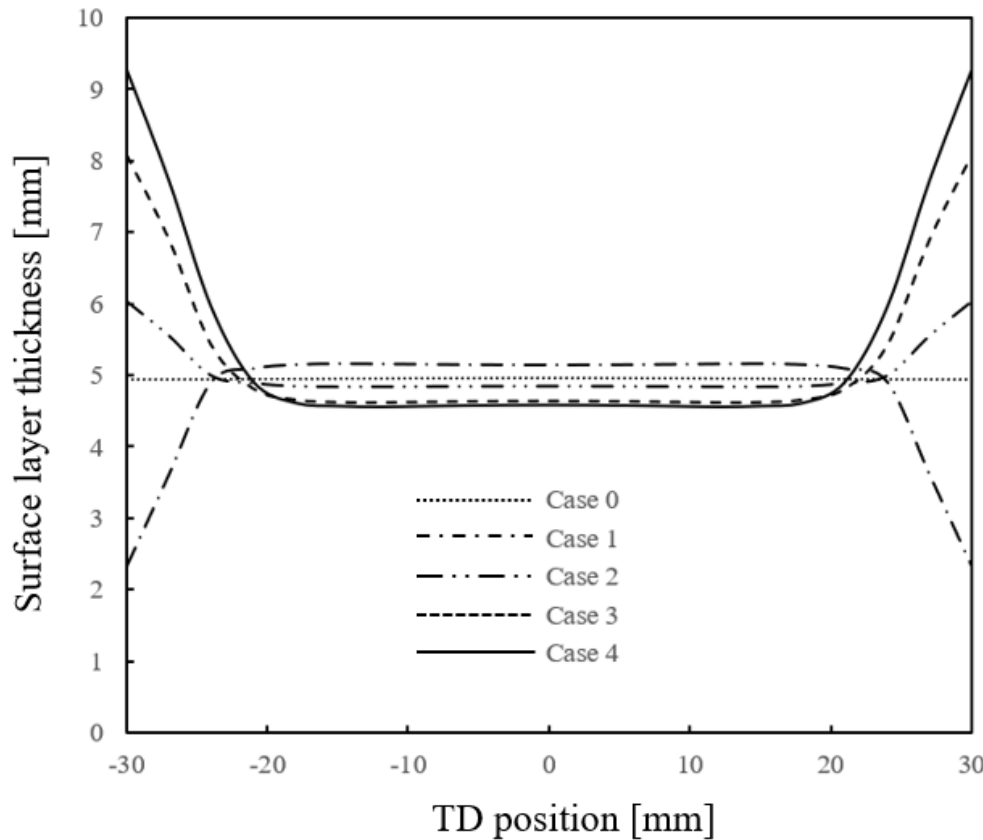


**Table 1 Second normal difference coefficients of PEM**

Case	Second normal stress difference coefficient : $\psi_2$ [Pa · s <sup>2</sup> ]		
	Layer 1	Layer 2	Layer 3
0	0	0	0
1	0	-60	0
2	-8	-60	-8
3	-10	-60	-10
4	-18	-60	-18

LDPE (LC720,LF405M)  
supplied by Japan Polyethylene Corp.

**Fig.17 Flow curve fitted using the Cross model**



$\psi_2 [Pa \cdot s^2]$	Layer1	Layer2	Layer3
Case4	-18	-60	-18
Case1	0	-60	0
Case0	0	0	0

**Fig. 18 Predicted surface layer thickness at the outlet position (B-B') of the feed block channel under the flat condition**

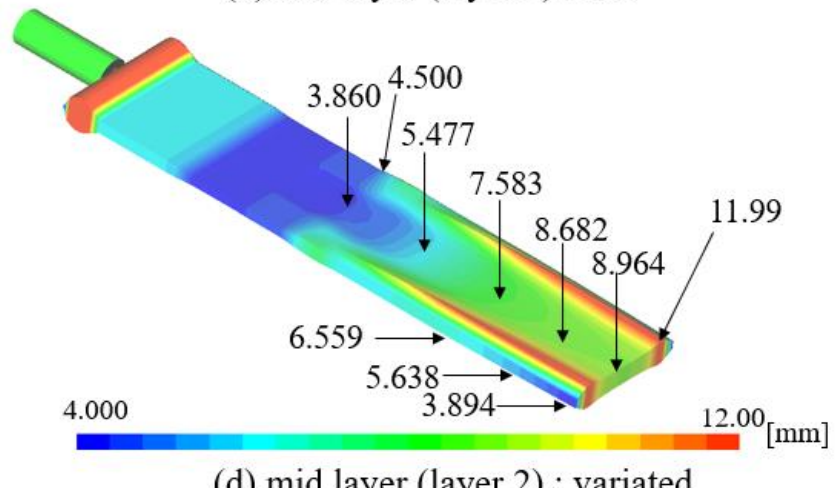
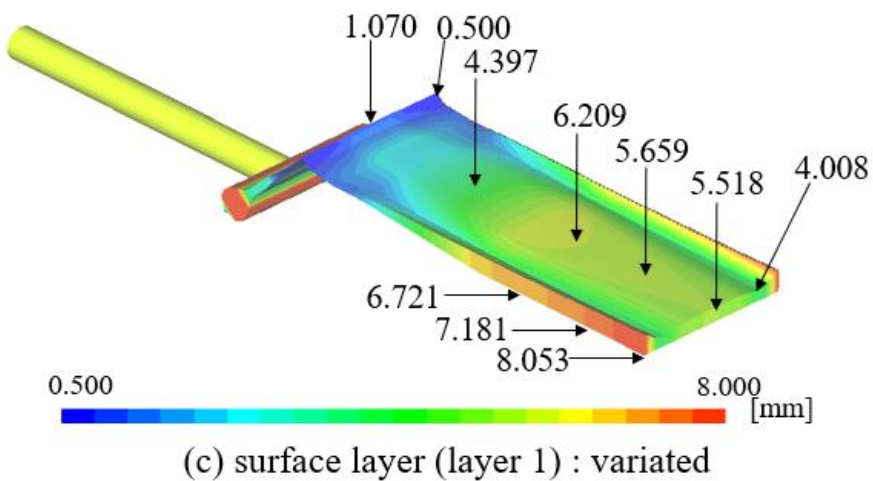
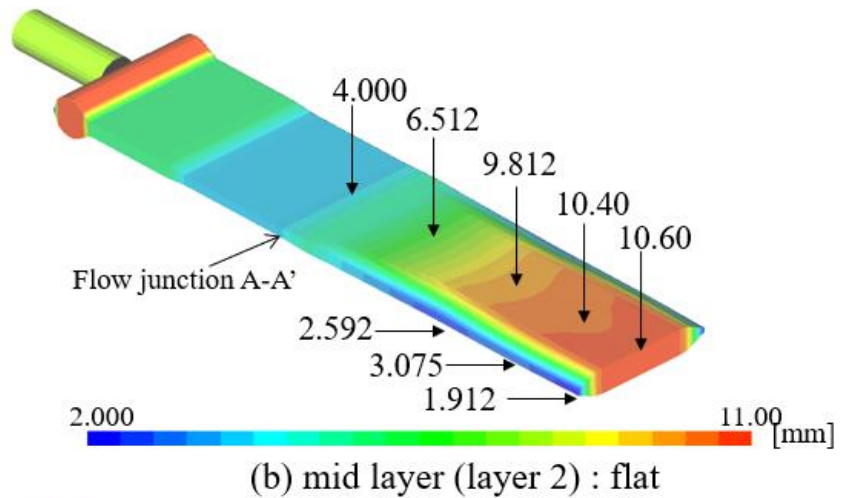
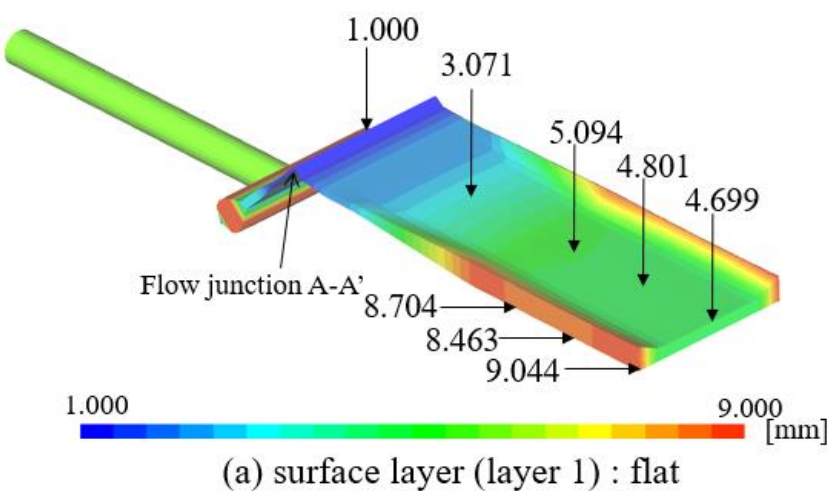
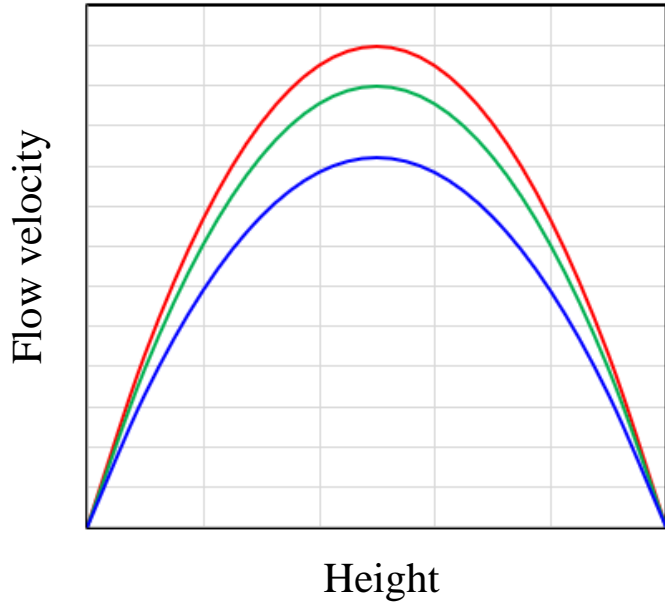


**Fig. 19 Predicted layer thickness ((a) surface layer, (b) mid layer : flat and (c) surface layer, (d) mid layer : variated)**

# Mysterious nature of multi layer flow

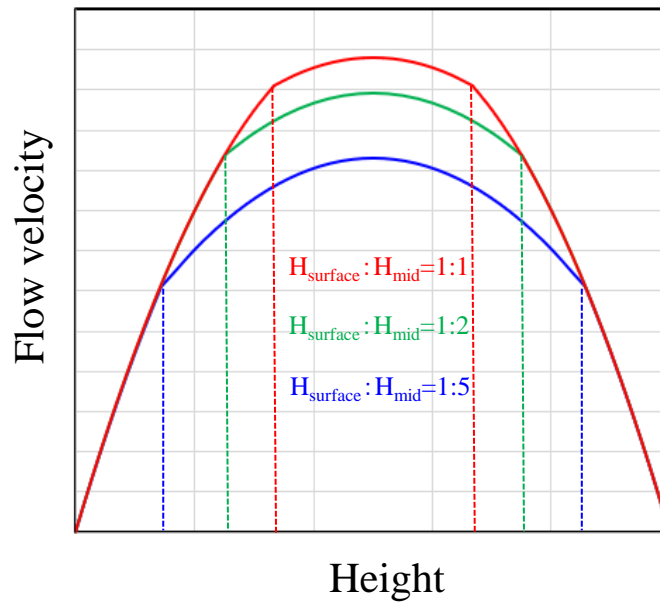
Mono layer flow



$$\Delta p < \Delta p < \Delta p$$

$$\therefore \Delta p = \frac{2\eta \dot{\gamma}_w}{H}$$

Multi layer flow ( $\eta_{surface} < \eta_{mid}$ )



$$\Delta p = \Delta p = \Delta p !!!$$

$$\chi_h^4 = -4\chi_\eta\chi_h^3 - 3(\chi_\eta - \chi_q\chi_\eta)\chi_h^2 + 4\chi_q\chi_\eta\chi_h + \chi_q\chi_\eta^2$$

for two layer flow under fully developed state

$$\frac{\partial}{\partial x_i} \left( S_l \frac{\partial p_l}{\partial x_i} \right) = F_l \quad \Rightarrow \quad v_{mi} \frac{\partial \chi_{qlm}}{\partial x_i} = 0$$

Elliptic type	$p_l = p$ for $l = 1 \sim n$	hyperbolic type
Diffusion		Convection

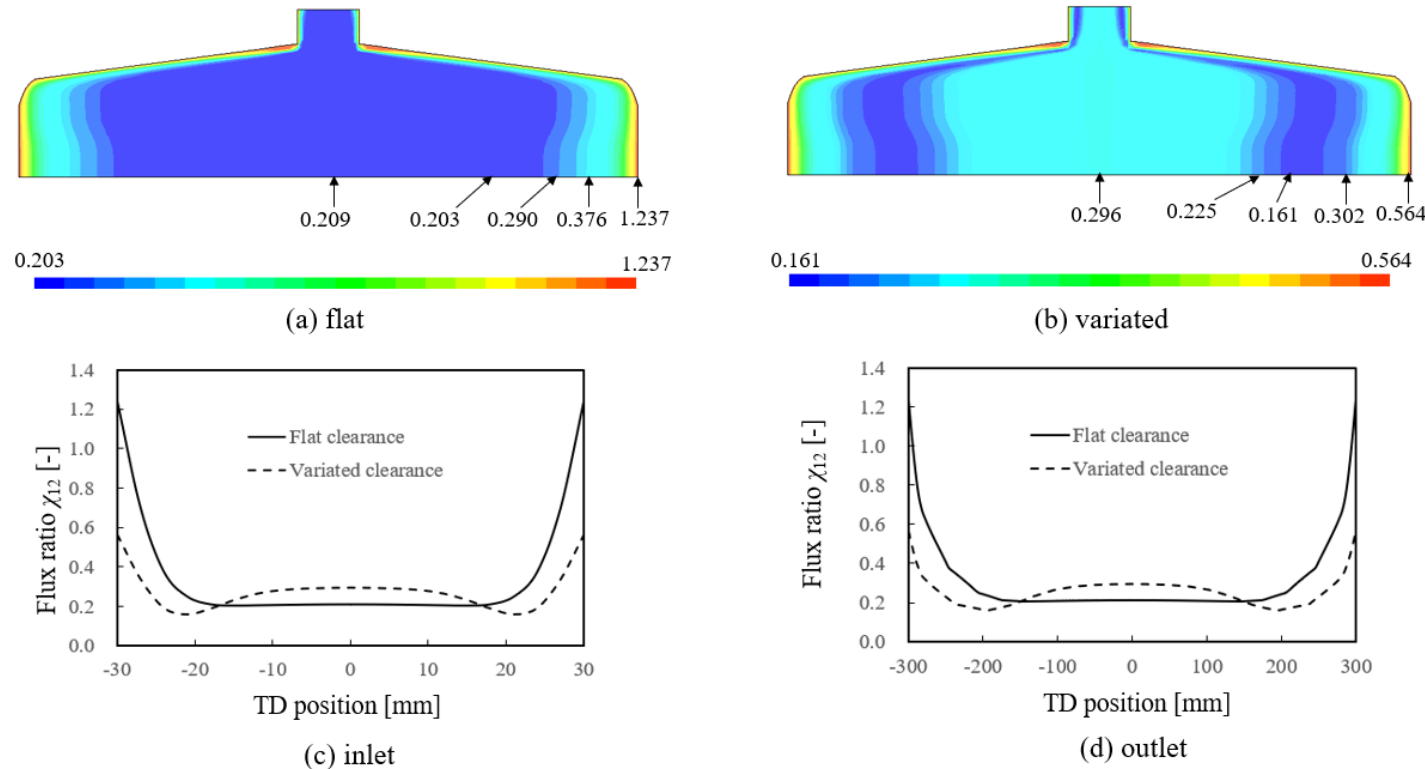


**Fig. 20 Predicted flux ratio  $\chi_{12}(= q_1/q_2 = \chi_{32})$  : contour plot of (a) flat and (b) variated , graph plot of (c) inlet (B-B') and (d) outlet (C-C')**

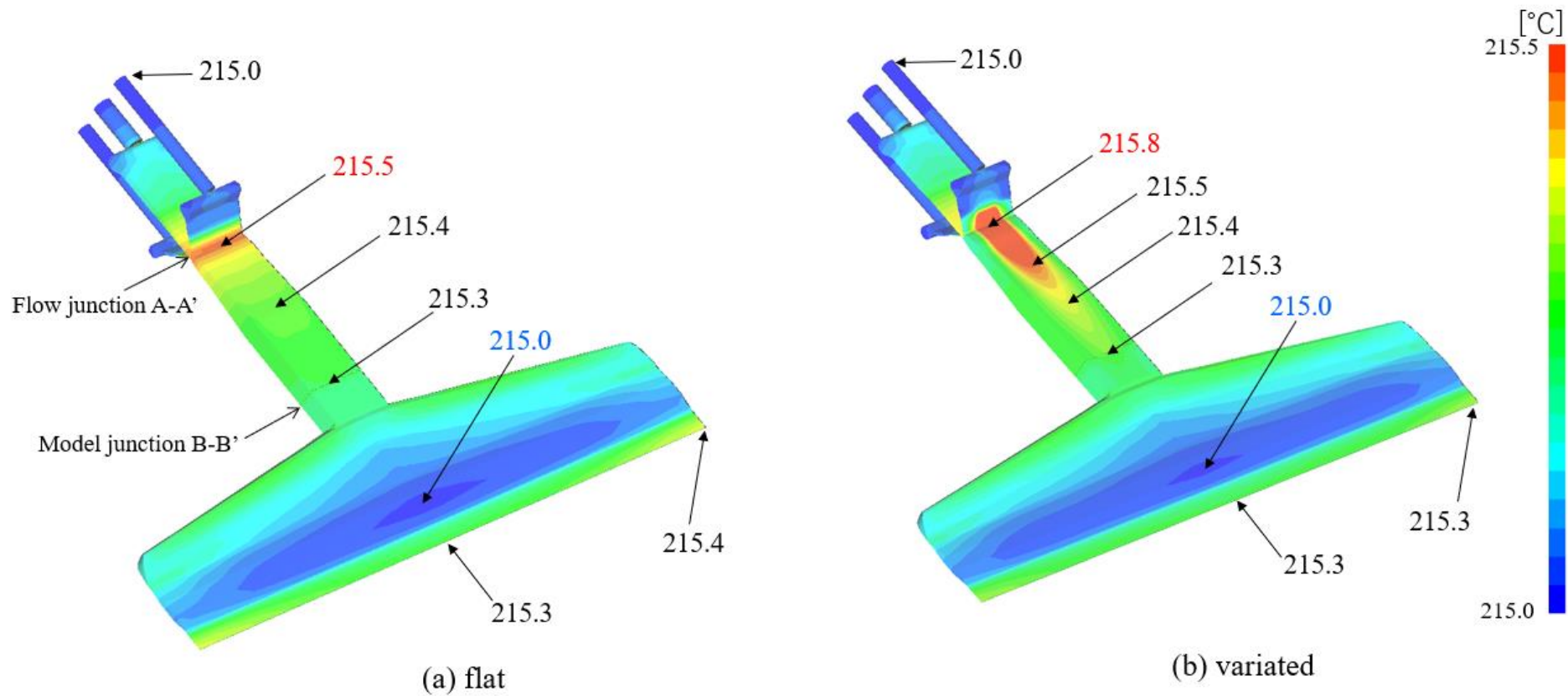
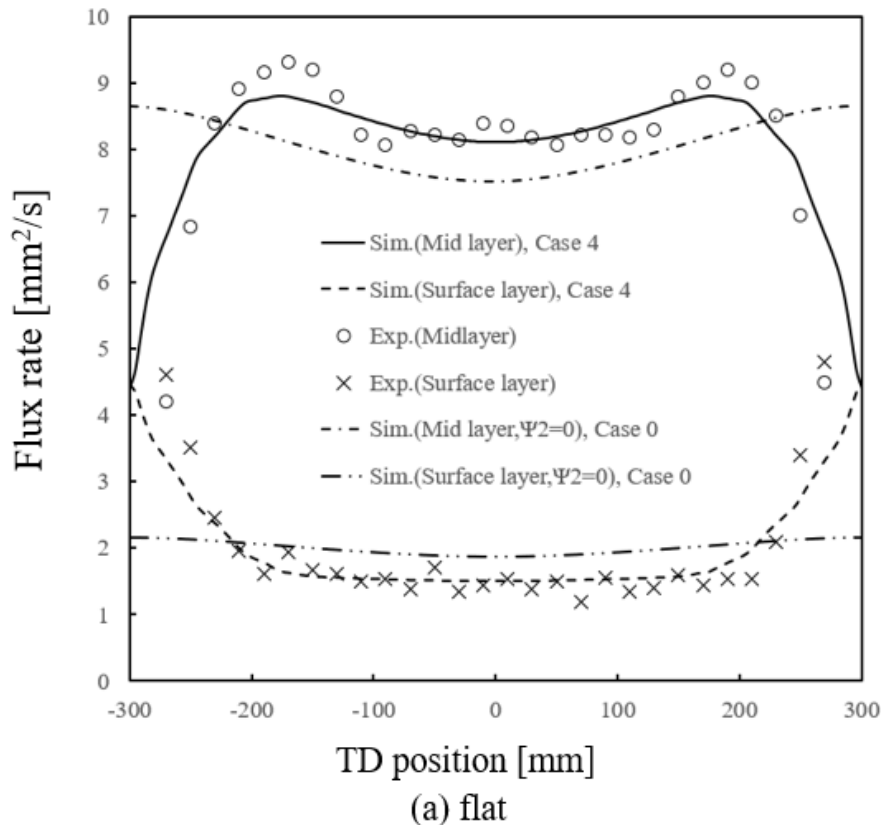
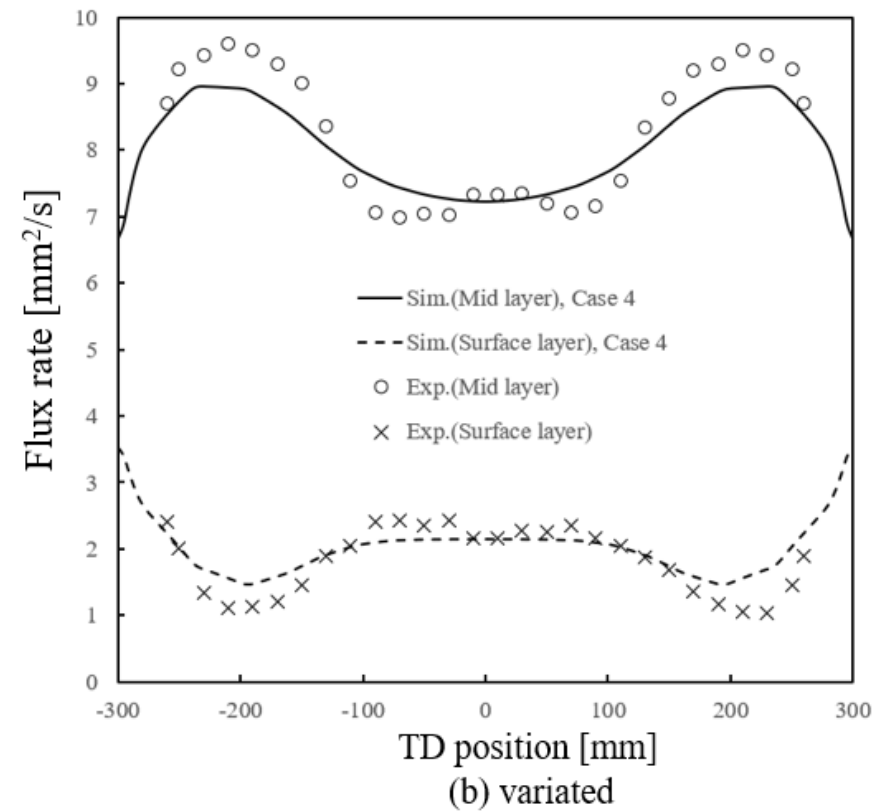


**Fig. 21 Comparison of the predicted pressure  
((a) flat and (b) variated)**



(a) flat



(b) variated

**Fig. 22 Comparison of the measured and the predicted flux rate at the die outlet position (C-C'), ((a) flat and (b) variated)**

- Various phenomena in the polymer extrusion process can be quantified in a short computational time with an easy operation using 2.5D FEM.
- The unfilled state in the twin screw extruder can be represented with moderate accuracy by the pressure rearrangement algorithm.
- The implementation of PEM reduces the discrepancy between the predicted layer thickness and the measured value in a feed block type coat hanger die.

## 「 Experimental Investigation and Numerical Simulation of a Self-Wiping Corotating Parallel Octa-Screw Extruder 」<sup>5)</sup>

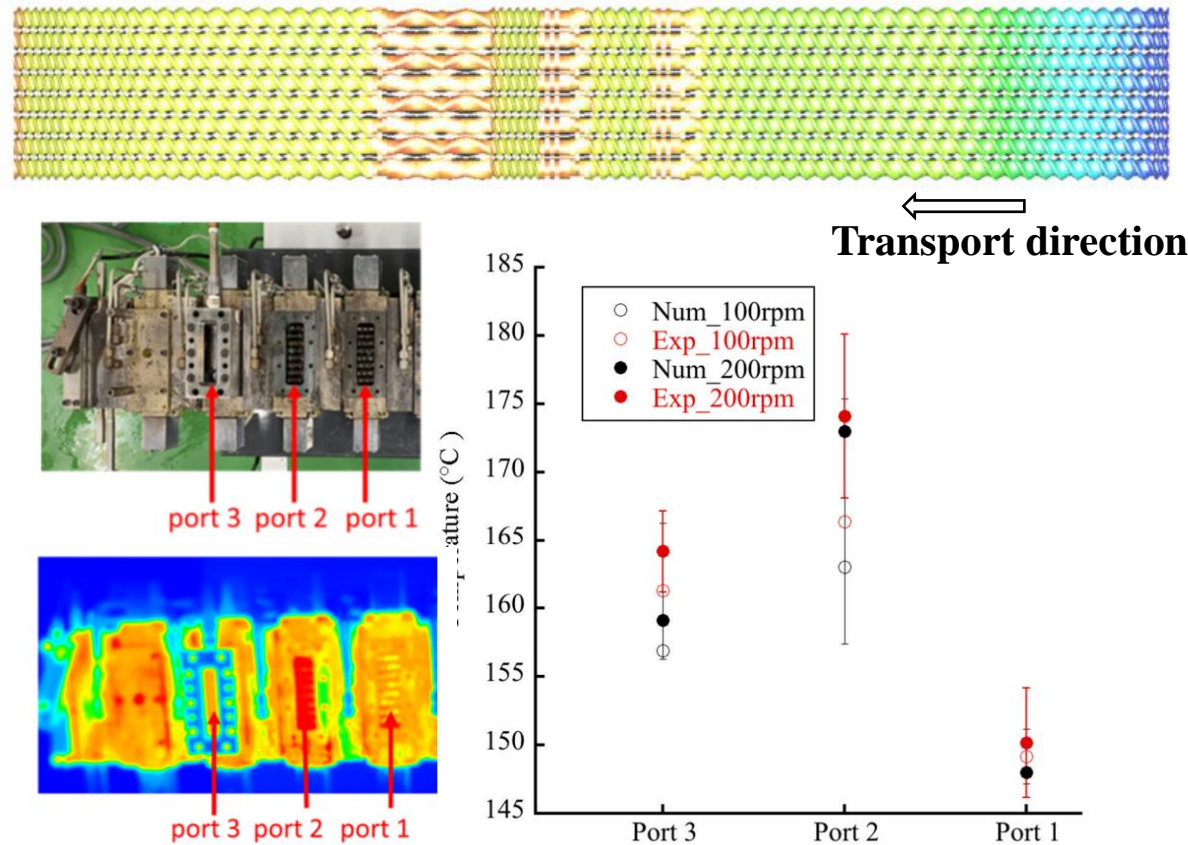


Fig. 23 Measured and calculated temperature distribution in an octa screw extruder

# Experimental verifications and enhancement of applications

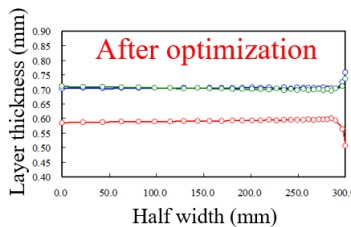
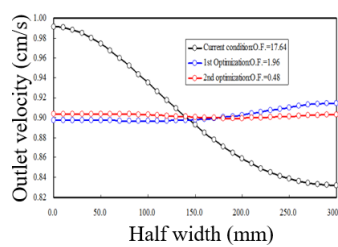
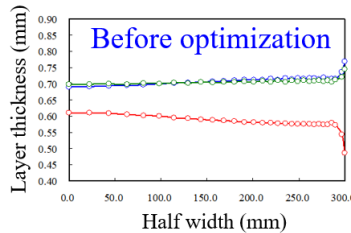
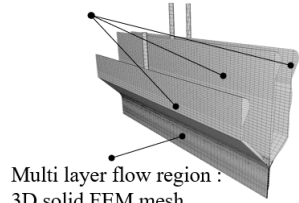
## For screw extruder



Side feed, Reactive extrusion, etc.

## For multilayer extrusion die

Mono layer flow region :  
2.5D Hele-Shaw FEM mesh



Optimization analysis of a multi manifold die

